

Observation of Au_2H^- impurity in pure gold clusters and implications for the anomalous Au-Au distances in gold nanowires

Hua-Jin Zhai, Boggavarapu Kiran, and Lai-Sheng Wang^{a)}

*Department of Physics, Washington State University, Richland, Washington 99352
and W. R. Wiley Environmental Molecular Sciences Laboratory, Pacific Northwest National Laboratory,
Richland, Washington 99352*

(Received 12 July 2004; accepted 11 August 2004)

Au_2H^- was recognized and confirmed as a minor contamination to typical photoelectron spectra of Au_2^- , produced by laser vaporization of a pure Au target using an ultrahigh purity helium carrier gas. The hydrogen source was shown to be from trace H impurities present in the bulk gold target. Carefully designed experiments using H_2^- and D_2^- -seeded helium carrier gas were used to study the electronic structure of Au_2H^- and Au_2D^- using photoelectron spectroscopy and density functional calculations. Well-resolved photoelectron spectra with vibrational resolution were obtained for Au_2H^- and Au_2D^- . Two isomers were observed both experimentally and theoretically. The ground state of Au_2H^- turned out to be linear with a terminal H atom [Au-Au-H^- ($^1\text{A}_1, \text{C}_{\infty v}$)], whereas a linear [Au-H-Au^- ($^1\text{A}_1, \text{D}_{\infty h}$)] structure with a bridging H atom was found to be a minor isomer 0.6 eV higher in energy. Calculated electron detachment energies for both isomers agree well with the experimental spectra, confirming their existence in the cluster beam. The observation and confirmation of H impurity in pure gold clusters and the 3.44 Å Au-Au distance in the [Au-H-Au^-] isomer presented in the current work provide indirect experimental evidence that the anomalous 3.6 Å Au-Au distances observed in gold nanowires is due to an “invisible” hydrogen impurity atom.

© 2004 American Institute of Physics. [DOI: 10.1063/1.1802491]

I. INTRODUCTION

During the past decade, gold has become the subject of active research in nanoelectronics,^{1–20} biosciences,²¹ catalysis,^{22–24} and cluster science.^{25–35} One of the exciting developments was the fabrication of gold nanowires one atom thick,^{1–6} which are the thinnest nanocontacts. Atomic-thick nanowires were exclusively observed for 5*d* metals,^{7,8} and strong relativistic effects were believed to play vital roles.²⁵ These monoatomic gold nanowires were observed to be exceptionally stable, reaching interatomic distances as large as 3.6 Å,^{1–5} a value significantly larger than the equilibrium Au-Au distance in gold dimer (2.48 Å) and in bulk fcc gold (2.88 Å). Several proposals have been put forth to interpret the abnormally high Au-Au distances.^{11–20} Among the previous proposals is the existence of undetected impurity atoms,^{5,18–20} such as H, B, C, CC, N, O, and S. However, all the impurities except H have been shown to give Au-Au distances much larger than 3.6 Å. Two recent theoretical works^{19,20} concluded that H is the best and only candidate for the 3.6 Å Au-Au distance. However, there has been no direct experimental observation of any impurity atoms in the monoatom gold nanowires.

We have been interested in probing the electronic structure and chemical bonding of gold clusters^{32–35} using anion photoelectron spectroscopy (PES). During our experiment on Au_2^- , we noticed a mysterious PES band at ~3.6 eV, which appeared in the HOMO-LUMO (HOMO and LUMO are highest occupied and lowest unoccupied molecular orbitals,

respectively) gap region of Au_2^- .³³ Upon examination of the literature, we found that the same feature was also present in several previous PES studies on Au_2^- .^{27–29} No convincing explanations for this feature have been put forth, despite exhaustive efforts.^{28,29} Recently, several experimental studies on gold hydride clusters have been reported.^{36–40} In particular, Gantefor and co-workers^{36,37} have reported PES spectra for a series of small gold hydride clusters accompanied with density functional theory (DFT) calculations. We noted that the binding energy of one of the PES features of Au_2H^- was very close to the mysterious band present in the Au_2^- PES spectra. This led to our suspicion that the origin of the mysterious band in the Au_2^- spectrum might be due to contamination from Au_2H^- .

In this work, we reexamined the PES spectra of Au_2^- and confirmed that the 3.6 eV band in the Au_2^- spectra was indeed due to the Au_2H^- contamination, despite the fact that a high purity Au target was used to produce the gold clusters. We carried out further experiment on Au_2H^- and Au_2D^- using H_2^- and D_2^- -seeded helium carrier gas and observed two isomers for the anions. Density functional theory calculations were performed to elucidate the structures and bonding of the anions and the neutral clusters and were compared with the experimental data. In agreement with previous DFT calculations,³⁶ we found that the ground state of Au_2H^- is linear [Au-Au-H^-] and there exists another linear isomer [Au-H-Au^-] ~0.6 eV higher in energy. The calculated electron binding energies of the two linear isomers agree well with the experimental data. The Au-H bond length was found to be 1.72 Å, giving a 3.44 Å Au-Au distance in the

^{a)}Electronic mail: ls.wang@pnl.gov

[Au-H-Au]⁻ cluster, very close to the abnormally long 3.6 Å Au-Au distance observed in the gold nanowires. The observation and confirmation of H impurity in pure gold clusters and the correct Au-H-Au distance presented in the current work provide indirect experimental evidence that the abnormal Au-Au distance observed in the gold atom wire are due to a hydrogen impurity atom.

II. EXPERIMENTAL METHOD

The experiments were carried out using a magnetic-bottle-type PES apparatus equipped with a laser vaporization supersonic cluster source, details of which have been described previously.^{41,42} Briefly, bare gold clusters were generated by laser vaporization of a pure gold target (99.99%) with ultrahigh purity helium as carrier gas (99.9999%). Au₂H⁻ and Au₂D⁻ clusters were produced using 0.5% H₂- or D₂-seeded helium carrier gas. Negatively charged clusters were produced from the source and analyzed using a time-of-flight mass spectrometer with a mass resolution of about $M/\Delta M = 350$ in the low mass range (<200 amu). The cluster species of interest was mass selected using a three-grid mass gate as described previously⁴¹ and decelerated before being photodetached. Three detachment photon energies were used in the current study: 532 nm (2.331 eV), 266 nm (4.661 eV), and 193 nm (6.424 eV). Photoelectrons were collected at nearly 100% efficiency by the magnetic bottle and analyzed in a 3.5 m long electron flight tube. Photoelectron spectra were calibrated using the known spectrum of Rh⁻, and the energy resolution of the apparatus was $\Delta Ek/Ek \sim 2.5\%$, that is, ~ 25 meV for 1 eV electrons.

III. EXPERIMENTAL RESULTS

A. Au₂H⁻ from pure Au target and pure He carrier gas

We first repeated the Au₂⁻ experiment using a pure Au target and pure He carrier gas, as we did before.³³ The spectra at 193 and 266 nm are shown in Fig. 1. The 193 nm spectrum is identical to that reported in Ref. 33. Nine main spectral features were observed and are labeled with the lowercase letters, *x, a–h*. The weak mysterious peak at ~ 3.6 eV was labeled as *X*. During this experiment, we set the mass gate to select the center part of the Au₂⁻ mass peak, as we usually do. To test if there would be any contamination due to Au₂H⁻ in the Au₂⁻ peak, we delayed the mass gate slightly to select the later part of the Au₂⁻ peak and took the data again, as shown in Figs. 1(c) and 1(d). We noted that the relative intensity of the 3.6 eV peak increased slightly. We then delayed the mass gate further to choose the tail part of the Au₂⁻ peak on the high mass side and obtained the spectra displayed in Figs. 1(e) and 1(f). To our surprise, the relative intensity of the 3.6 eV peak increased dramatically, accompanied by the appearance a very weak feature (*X'*) at ~ 2.8 eV and two features (*E, F*) at the high energy side. At the same time, the relative intensities of features *d* and *f* were also enhanced, suggesting that there were new features overlapping with them.

We noted that the binding energy of the 3.6 eV peak (*X*) was the same as that reported recently for Au₂H⁻.³⁶ Thus

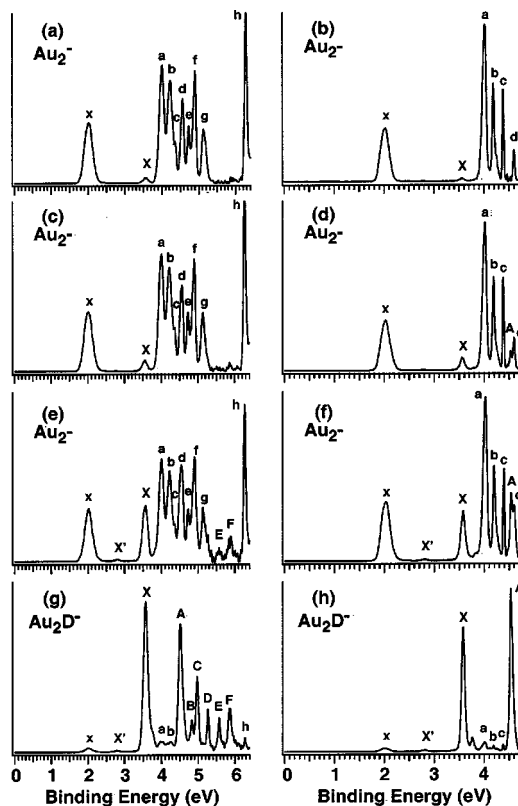


FIG. 1. Photoelectron spectra of Au₂⁻ and Au₂D⁻ at 193 nm (6.424 eV, left column) and 266 nm (4.661 eV, right column). (a)–(f) the spectra were taken with a pure gold target and ultrapure He carrier gas, but the mass gate timing was systematically varied to select the middle [(a),(b)], late [(c),(d)], and tail [(e),(f)] part of the Au₂⁻ mass peak. (g) and (h) photoelectron spectra of Au₂D⁻ produced by using a D₂-seeded He carrier gas. Features labeled with lower case letters (*x, a, b, c, d, e, f, g, h*) are due to Au₂⁻; features labeled with capital letters (*X', X, A, B, C, D, E, F*) are due to Au₂H⁻/Au₂D⁻, where *X'* indicates a feature from a minor isomer of Au₂H⁻/Au₂D⁻.

the additional features in Fig. 1(e) should all be due to Au₂H⁻. This observation clearly showed that there was a small amount of contamination from Au₂H⁻ in the Au₂⁻ mass peak. Our mass resolution was about 350, which was barely enough to resolve the Au₂H⁻ peak from that of Au₂⁻. However, because the Au₂H⁻ contamination was very slight and its abundance was extremely weak, we could not observe a separate Au₂H⁻ peak, which was simply buried in the tail of the Au₂⁻ peak on the higher mass side. This is why the hydride contamination has never been recognized previously. Furthermore, because of the close proximity of the two mass peaks and the finite peak width, we could not cleanly mass select one or the other and would always obtain a mixture of the two, although their relative proportions can be changed by changing the mass gate timing. We should also point out that Au₂⁻ was the only mass peak contaminated with the hydride. We checked Au₃⁻ and several larger Au_n⁻ clusters and found no detectable hydride contamination in their PES spectra. In addition, since ultrapure He carrier gas (99.9999%) was used and no contamination was ever observed in other cluster experiments with this carrier gas, we suspect the hydrogen contamination came from trace

amount of hydrogen impurity in the gold target, which has a specified purity of 99.99%.

B. Au₂H⁻ and Au₂D⁻ from H₂- and D₂-seeded He carrier gases

To verify the above observation, we produced Au₂H⁻ using a H₂-seeded He carrier gas. We obtained spectra similar to those shown in Figs. 1(e) and 1(f) because the Au₂⁻ mass peak was always dominating and the Au₂H⁻ peak could not be cleanly mass gated, as discussed above. To further confirm the observation of Au₂H⁻, we also performed experiments using a D₂-seeded He carrier gas, as shown in Figs. 1(g) and 1(h). Because of the 2 amu separation between Au₂D⁻ and Au₂⁻, it could be mass gated more cleanly, although a small amount of Au₂⁻ was still discernible in the spectra of Au₂D⁻. But the main spectral features in Figs. 1(g) and 1(h) are due to Au₂D⁻ and they are identical to those observed for Au₂H⁻ (the isotope shift on the electron binding energy was expected to be much smaller than our instrumental resolution). In addition to the three strong features (*X*, *E*, *F*) observed in Fig. 1(e) for Au₂H⁻, four more features (*A*, *B*, *C*, *D*) were identified in Fig. 1(g). These features were overlapped with those from Au₂⁻ in the case of Au₂H⁻ [Fig. 1(e)]. A very weak band *X'* was also observed in the spectra of Au₂D⁻, identical to that in the spectra of Au₂H⁻ [Figs. 1(e) and 1(f)]. The *X'* feature was extremely weak for both Au₂H⁻ and Au₂D⁻, but was always present. It was attributed to a minor isomer and was born out from the theoretical calculations, as shown below.

C. "Clean" spectra for Au₂D⁻ and Au₂⁻

We obtained "clean" spectra for Au₂D⁻ and Au₂⁻ by subtracting the respective contaminations. These spectra are shown in Figs. 2 and 3 for Au₂D⁻ and Au₂⁻, respectively. The ground state transition (*X*) of Au₂D⁻ was clearly vibrationally resolved with a frequency of 1470 (50) cm⁻¹. Such a high frequency is likely due to the Au-D stretching vibration. In the inset of Fig. 2, we compared the vibrational structures of Au₂D⁻ and Au₂H⁻. There is a clear isotope shift and the vibrational frequency estimated for Au₂H is 2050 (100) cm⁻¹ from our data. Our obtained vibrational frequencies for Au₂D and Au₂H compare well with the vibrational frequencies for the diatomics, AuD (1635.0 cm⁻¹) and AuH (2305.0 cm⁻¹),⁴³ and the isotope shift factor (ν_D/ν_H) is identical for both systems. In Fig. 2, the weak feature *X'* is expanded and is more clearly shown. Despite its weak intensity, good signal to noise was obtained due to the high count rates. The adiabatic detachment energy (ADE) and vertical detachment energy (VDE) for the *X'* band were measured to be 2.73 and 2.81 eV, respectively. The binding energies for all the observed spectral transitions for Au₂D⁻ are given in Table I. Since no measurable differences were observed for the electron binding energies for Au₂D⁻ and Au₂H⁻, all the values given in Table I can also be taken for Au₂H⁻, for which DFT calculations were done (see below).

In Fig. 3, the 532 nm spectrum of Au₂⁻ is also shown, which is partially vibrationally resolved with an estimated spacing of 190 ± 15 cm⁻¹. A previous PES study by

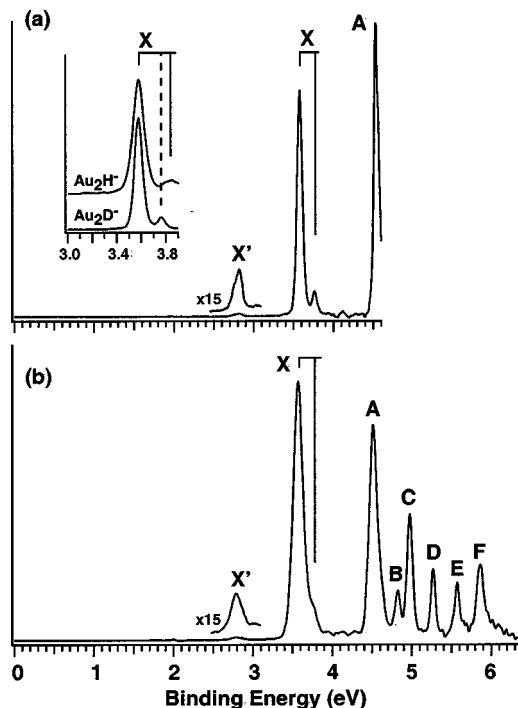


FIG. 2. Photoelectron spectra of pure Au₂D⁻ after weighted subtraction of the Au₂⁻ components. (a) 266 nm (4.661 eV); (b) 193 nm (6.424 eV). The inset compares the vibrational structures of the ground state transitions of Au₂H⁻ and Au₂D⁻. Although there is no measurable isotope shift on the electronic binding energies for Au₂H⁻ and Au₂D⁻, the isotope shift on the vibrational structure is huge.

Lineberger and co-workers²⁶ yielded an accurate vibrational frequency for Au₂, 190.9 cm⁻¹, which is barely within our instrumental resolution. As shown in Fig. 3, nine well-resolved features (*x*, *a*, *b*, *c*, *d*, *e*, *f*, *g*, *h*) were obtained (Table II), revealing eight low-lying excited states for neutral Au₂. Several of these states have been identified and assigned previously using resonant two-photon ionization spectroscopy by Bishea and Morse,⁴⁴ as shown in Table II. These optically-identified excited states have been compared with PES data previously by Handschuh *et al.*²⁸ The current PES data are consistent with those of Handschuh *et al.* except that one additional state (*h*) was observed at the very high binding energy side in the current 193 nm spectrum [Fig. 3(c)]. Thus, Fig. 3 represents the heretofore most complete PES data set for Au₂⁻. These spectroscopic data will be valuable in benchmarking theoretical calculations on gold clusters.

IV. DENSITY FUNCTIONAL CALCULATIONS

Density functional calculations were carried out to elucidate the structural and electronic properties of Au₂H⁻ and Au₂H. Calculations were done using the generalized gradient approach with the Perdew–Wang exchange–correlations functional.⁴⁵ Scalar relativistic effects were calculated at the zero-order regular approximation Hamiltonian⁴⁶ along with the triplet-zeta plus *p*- and *f*-polarization functions (TZ2P) for the valance orbitals of Au and H atoms. Additionally, the frozen core (1s²-4f¹⁴) approximation was used for Au atoms in the calculations. Vertical detachment energies for the anion were calculated via the self-consistent field energy dif-

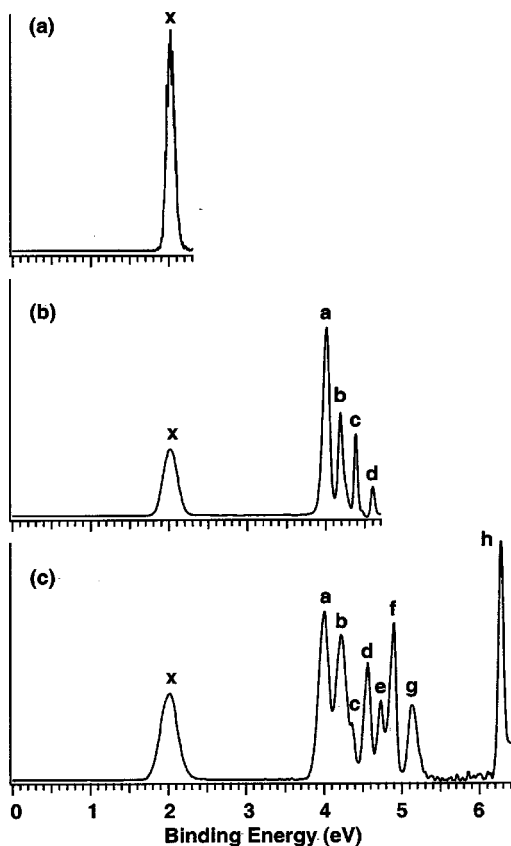


FIG. 3. Photoelectron spectra of Au_2^- after weighted subtraction of the Au_2H^- contamination. (a) 532 nm (2.331 eV); (b) 266 nm (4.661 eV); (c) 193 nm (6.424 eV).

ference between neutral and anion states. All calculations were done by the Amsterdam Density Functional (ADF 2002) program.⁴⁷

The optimized structures for Au_2H^- and Au_2H are summarized in Fig. 4. The anion ground state turned out to be linear $[\text{Au}-\text{Au}-\text{H}]^-$ [Fig. 4(a), $C_{\infty v}$, 1A_1]. A linear isomer $[\text{Au}-\text{H}-\text{Au}]^-$ [Fig. 4(b), $D_{\infty h}$, 1A_1] was found 0.60 eV higher in energy. These results are in agreement with a previous DFT study on Au_2H^- .³⁶ The neutral Au_2H ground

TABLE I. Observed vertical (VDE) and adiabatic (ADE) detachment energies for Au_2H^- , along with theoretical results from DFT calculations.

Observed feature	ADE (eV)		VDE (eV)	
	Expt. ^a	Theo.	Expt. ^a	Theo.
X^b	3.55 (3)	3.20 ^c	3.57 (2)	3.31
<i>A</i>			4.52 (2)	4.37
<i>B</i>			4.82 (3)	4.51
<i>C</i>			4.97 (3)	4.75
<i>D</i>			5.27 (3)	
<i>E</i>			5.57 (3)	
<i>F</i>			5.86 (3)	
X'	2.73 (5)	2.56	2.81 (3)	2.76

^aNumbers in parentheses represent experimental uncertainties in the last digit.

^bGround state vibrational frequencies for the Au_2H and Au_2D neutrals were measured to be 2050 (100) cm^{-1} and 1470 (50) cm^{-1} , respectively (Fig. 2).

^cADE from structure (a) to structure (c) in Fig. 4, which defines the theoretical adiabatic electron affinity of Au_2H .

TABLE II. Observed adiabatic (ADE) and vertical (VDE) detachment energies for Au_2^- and comparison to previously identified excited states of Au_2^- .

PES feature	ADE (eV) ^{a,b}	VDE (eV) ^{a,b}	Excitation energy (eV) ^{a,c}	T_0 (eV) ^d	Assignment ^e
x^f	1.94 (2) ^g	2.01 (2)	0.00	0.00	$X^1\Sigma_g^+$
<i>A</i>	3.96 (3)	4.01 (2)	2.02	2.06	$a^3\Sigma_u^+(1_u)$
<i>b</i>	4.16 (3)	4.19 (2)	2.22	2.25	$A^1\Gamma_u$
<i>c</i>	4.37 (3)	4.38 (2)	2.43	2.43	$A^0\Gamma_u^+$
<i>d</i>	4.59 (3)	4.60 (2)	2.65		
<i>e</i>	4.72 (4)	4.73 (3)	2.78		
<i>f</i>	4.88 (4)	4.90 (3)	2.94	2.98	$B'(1_u)$
<i>g</i>	5.11 (4)	5.13 (3)	3.17	3.18	$B^0\Gamma_u^+$
<i>h</i>	6.26 (4)	6.27 (2)	4.32		

^aThis work.

^bNumbers in parentheses represent experimental uncertainties in the last digit.

^cObtained from the ADE difference between the excited states and the ground state of Au_2^- .

^dTerm values for the excited states of Au_2^- obtained from resonant two-photon spectroscopy (Ref. 44).

^eSee Ref. 44.

^fGround state vibrational frequency was measured to be 190 (15) cm^{-1} from Fig. 3(a). A more accurate value was reported previously, 190.9 cm^{-1} (Ref. 26).

^gA more accurate ADE value was reported previously, 1.938 ± 0.007 eV (Ref. 26).

state was triangular [Fig. 4(c), C_{2v} , 2B_2], in which the H atom bridges the Au-Au atoms. The linear Au-Au-H and Au-H-Au neutral species were located 0.10 and 0.17 eV higher, respectively. Frequency analyses showed that the linear $[\text{Au}-\text{Au}-\text{H}]^-$ and $[\text{Au}-\text{H}-\text{Au}]^-$ anions and the triangular Au_2H neutral were all true minima in the potential energy surfaces, whereas the neutral Au-Au-H and Au-H-Au species were second-order saddle points each with two imaginary frequencies. The calculated detachment energies for both isomers of Au_2H^- are listed in Table I, where they are compared with experimental PES data.

V. DISCUSSION

A. Spectral assignments

Two linear structures, $[\text{Au}-\text{Au}-\text{H}]^-$ and $[\text{Au}-\text{H}-\text{Au}]^-$ were identified in our DFT calculations for Au_2H^- (Fig. 4),

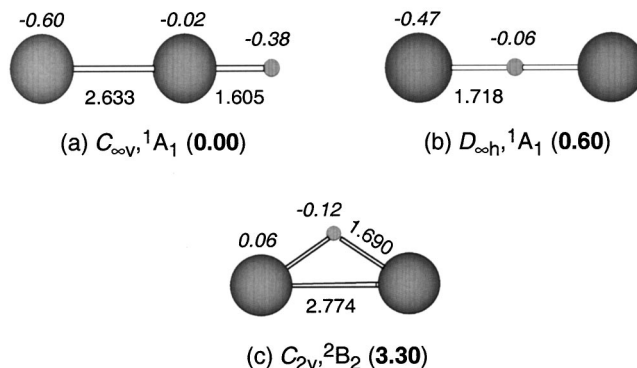


FIG. 4. Optimized ground state structure (a) and a low-lying isomer (b) for the Au_2H^- anion, and the ground state structure (c) for the Au_2H neutral. Bond lengths are in Å, and relative energies in eV are given in parentheses. Shown in *italic* is the Mulliken charge distribution.

where the lowest energy structure contains a terminal H atom and the structure with a bridging H atom is a low-lying isomer 0.6 eV higher in energy. These theoretical results are consistent with our experimental observation that both the spectra of Au₂H⁻ and Au₂D⁻ appeared to contain a weakly populated isomer (*X'* in Figs. 1 and 2). To facilitate quantitative comparison with the experimental data, ADEs and VDEs for both the [Au-Au-H]⁻ and [Au-H-Au]⁻ linear anions were calculated. For the lowest energy isomer, we also calculated VDEs for several higher binding energy detachment channels. The theoretical results are compared with the experimental data in Table I. The calculated ADE for the ground state anion is 3.20 eV, compared with the experimental value of 3.55 eV. The calculated ADE for the low-lying isomer is 2.56 eV, much lower than that of the ground state anion, in good agreement with the measured ADE for the feature *X'* at 2.73 eV. Overall, the calculated VDEs for both isomers are in good agreement with the measured PES spectra (Table I), firmly establishing that both isomers were present in our mass selected Au₂H⁻ (Au₂D⁻) cluster beam, with the [Au-H-Au]⁻ isomer as a minor species. Considering the relatively high energy of this isomer, it was surprising that it was observed at all, suggesting that there is likely to be a significant energy barrier between the two isomers. The observation of the minor isomer was also due to our relatively high count rates and good counting statistics. We note that this isomer was not observed in the previous PES study on gold hydride clusters.³⁶

B. Anion-to-neutral structural change for [Au-Au-H]⁻ and [Au-Au-D]⁻

Neutral Au₂H has a triangular structure, which is very different from the linear structures found for the Au₂H⁻ anion. Thus the Au₂H⁻/Au₂H systems are similar to the coinage metal trimers (Au₃, Ag₃, and Cu₃), whose anions are all linear while their neutral ground states are all triangular.⁴⁸⁻⁵¹ The leading PES band (*X*) of Au₂H⁻/Au₂D⁻ was sharp with a rather steep onset and exhibited a short vibrational progression in the Au-H/D stretching mode (Fig. 2). This observation seemed not to be consistent with the large anion-to-neutral geometry change from the DFT calculations (Fig. 4). Previous PES studies on the coinage metal trimers showed that there is a large difference between the ADE and VDE for Cu₃⁻ and the ADE-VDE difference becomes smaller in Ag₃⁻.²⁶ Our previous PES study showed that the ground state transition in Au₃⁻ was extremely sharp and the peak width was within our instrumental resolution.³³ This is likely due to the fact that the energy difference in the neutral cluster between the linear and triangular structures is small for Au₃. In the Au₂H case, our calculation showed that the triangular structure is only more stable than the linear saddle point by 0.10 eV, which is the same as the difference between the neutral triangular and linear structure of Au₃.⁵⁰ In addition, the potential energy surface along the bending coordinate of Au₂H is likely to be rather flat. Since photodetachment is a vertical process, only the flat-top portion of the neutral potential energy surface of Au₂H along the bending coordinate is accessed upon photodetachment of Au₂H⁻, resulting in a narrow PES band. Therefore, the onset of the observed *X*

band, after taking into account of instrumental resolution, might not represent the adiabatic electron affinity of the neutral. But rather, it represented the upper limit of the adiabatic electron affinity. This can be seen from comparison between the experimental and theoretical ADE and VDE. For the [Au-Au-H]⁻ isomer, the difference between the calculated VDE and ADE is 0.11 eV, whereas the experimental VDE and ADE are nearly the same, suggesting that the experimental ADE in the current case is only a threshold value, which is the upper limit of the true adiabatic detachment energy. The same is true for the [Au-H-Au]⁻ isomer (Table I).

The difference between the anion and neutral ground state structures for Ag₃ has been exploited in so-called NeNePo (negative to neutral to positive⁵²) experiments to probe the relaxation dynamics from linear to triangular Ag₃ upon photodetachment of Ag₃⁻.^{48,49} The Au₂H⁻/Au₂D⁻ anions may provide even better systems for similar NeNePo experiments, which will essentially probe the motion of a H atom around a Au₂ dimer. The H/D substitution should also allow isotopic effect to be probed for the relaxation dynamics.

C. Implication of the observation of Au₂H⁻ impurity to the anomalous Au-Au distance in gold nanowires

The observation of the impurity cluster Au₂H⁻ using a highly pure Au target was totally unexpected in our cluster beam experiment, as well as in several previous studies. It should be noted that this was an exception among many studies on transition metal clusters in our laboratory. We confirmed that the hydrogen source comes from the Au target itself, i.e., the trace amount of H impurity in the Au target. Our observation suggests that it should not be too surprising that H may appear as an impurity in the gold nanowires. Our calculated Au-Au distance in the [Au-H-Au]⁻ isomer is 3.44 Å, which is very close to the anomalous Au-Au distance observed in gold nanowires. Both the observation of the Au₂H⁻ impurity from a pure gold target and the correct Au-Au distance in the [Au-H-Au]⁻ cluster provide strong, albeit indirect, evidence that H is the “invisible” atom that gives the anomalous Au-Au distance in gold nanowires.

VI. CONCLUSIONS

In conclusion, we demonstrated that a weak feature that appeared in the energy gap region of the photoelectron spectra of Au₂⁻ was in fact due to contamination from Au₂H⁻. We confirmed that the Au₂H⁻ contamination originates from trace H impurity of the gold target used in the laser vaporization cluster source. Photoelectron spectra were further obtained for Au₂H⁻ and Au₂D⁻ produced using H₂- and D₂-seeded He carrier gases, respectively. Two isomers were observed in the photoelectron spectra of Au₂H⁻ and Au₂D⁻. Density functional calculations were carried out to elucidate the structures of Au₂H⁻ and help interpret the experimental data. We found that Au₂H⁻ has a [Au-Au-H]⁻ linear ground state with a [Au-H-Au]⁻ low-lying isomer 0.6 eV higher in energy. The calculated electron binding energies of the two isomers agree well with the experimental observations, confirming the existence of the two isomers in the experimental

cluster beam. The calculated Au-Au distance in the $[\text{Au-H-Au}]^-$ isomer is 3.44 Å. The current experimental and theoretical study provides the first convincing, though indirect, evidence that the anomalous 3.6 Å Au-Au distance observed in monoatomic gold nanowires¹⁻⁵ should be due to the Au-H-Au bridge with an invisible H atom. This result also supports the latest theoretical calculations, which explored in detail the unique properties of gold hydride monoatomic nanowires and convincingly established the characteristic Au-Au distance of ~ 3.6 Å computationally.^{19,20} The invisible H in the gold nanowires is suggested to simply come from the trace H impurity present in bulk gold.

ACKNOWLEDGMENTS

This work was supported by the National Science Foundation (CHE-0349426) and performed at the W. R. Wiley Environmental Molecular Sciences Laboratory, a national scientific user facility sponsored by the Department of Energy's Office of Biological and Environmental Research and located at the Pacific Northwest National Laboratory, operated for DOE by Battelle.

- ¹H. Ohnishi, Y. Kondo, and K. Takayanagi, *Nature (London)* **395**, 780 (1998).
- ²A. I. Yanson, G. R. Bollinger, H. E. van den Brom, N. Agrait, and J. M. van Ruitenbeek, *Nature (London)* **395**, 783 (1998).
- ³C. Untiedt, A. I. Yanson, R. Grande, G. Rubio-Bollinger, N. Agrait, S. Vieira, and J. M. van Ruitenbeek, *Phys. Rev. B* **66**, 085418 (2002).
- ⁴V. Rodrigues and D. Ugarte, *Phys. Rev. B* **63**, 073405 (2001).
- ⁵S. B. Legoas, D. S. Galvao, V. Rodrigues, and D. Ugarte, *Phys. Rev. Lett.* **88**, 076105 (2002).
- ⁶Y. Takai, T. Kawasaki, Y. Kimura, T. Ikuta, and R. Shimizu, *Phys. Rev. Lett.* **87**, 106105 (2001).
- ⁷R. H. M. Smit, C. Untiedt, A. I. Yanson, and J. M. van Ruitenbeek, *Phys. Rev. Lett.* **87**, 266102 (2001).
- ⁸S. R. Bahn and K. W. Jacobsen, *Phys. Rev. Lett.* **87**, 266101 (2001).
- ⁹E. Z. da Silva, A. J. R. da Silva, and A. Fazzio, *Phys. Rev. Lett.* **87**, 256102 (2001).
- ¹⁰D. Kruger, H. Fuchs, R. Rousseau, D. Marx, and M. Parrinello, *Phys. Rev. Lett.* **89**, 186402 (2002).
- ¹¹M. Okamoto and K. Takayanagi, *Phys. Rev. B* **60**, 7808 (1999).
- ¹²H. Hakkinen, R. N. Barnett, and U. Landman, *J. Phys. Chem. B* **103**, 8814 (1999).
- ¹³H. Hakkinen, R. N. Barnett, A. G. Scherbakov, and U. Landman, *J. Phys. Chem. B* **104**, 9063 (2000).
- ¹⁴L. De Maria and M. Springborg, *Chem. Phys. Lett.* **323**, 293 (2000).
- ¹⁵N. V. Skorodumova and S. I. Simak, *Comput. Mater. Sci.* **17**, 178 (2000).
- ¹⁶D. Sanchez-Portal, E. Artacho, J. Junquera, P. Ordejon, A. Garcia, and J. M. Soler, *Phys. Rev. Lett.* **83**, 3884 (1999).
- ¹⁷J. A. Torres, E. Tosatti, A. Dal Corso, F. Ercolessi, J. J. Kohanoff, F. D. Di Tolla, and J. M. Soler, *Surf. Sci.* **426**, L441 (1999).
- ¹⁸S. R. Bahn, N. Lopez, J. K. Nørskov, and K. W. Jacobsen, *Phys. Rev. B* **66**, R081405 (2002).
- ¹⁹N. V. Skorodumova and S. I. Simak, *Phys. Rev. B* **67**, R121404 (2003).
- ²⁰F. D. Novaes, A. J. R. da Silva, E. Z. da Silva, and A. Fazzio, *Phys. Rev. Lett.* **90**, 036101 (2003).
- ²¹R. Elghanian, J. J. Storhoff, R. C. Mucic, R. L. Letsinger, and C. A. Mirkin, *Science* **277**, 1078 (1997).
- ²²M. Haruta, *Catal. Today* **36**, 153 (1997).
- ²³M. Valden, X. Lai, and D. W. Goodman, *Science* **281**, 1647 (1998).
- ²⁴A. Sanchez, S. Abbet, U. Heiz, W. D. Schneider, H. Häkkinen, R. N. Barnett, and U. Landman, *J. Phys. Chem. A* **103**, 9573 (1999).
- ²⁵P. Pyykko, *Angew. Chem., Int. Ed.* **41**, 3573 (2002).
- ²⁶J. Ho, K. M. Ervin, and W. C. Linberger, *J. Chem. Phys.* **93**, 6987 (1990).
- ²⁷K. J. Taylor, C. L. Pettiette-Hall, O. Cheshnovsky, and R. E. Smalley, *J. Chem. Phys.* **96**, 3319 (1992).
- ²⁸H. Handschuh, G. Gantefor, P. S. Bechthold, and W. Eberhardt, *J. Chem. Phys.* **100**, 7093 (1994).
- ²⁹Y. Negishi, Y. Nakamura, A. Nakajima, and K. Kaya, *J. Chem. Phys.* **115**, 3657 (2001).
- ³⁰H. Hakkinen, M. Moseler, and U. Landman, *Phys. Rev. Lett.* **89**, 033401 (2002).
- ³¹F. Furche, R. Ahlrichs, P. Weis, C. Jacob, S. Gilb, T. Bierweiler, and M. F. Kappes, *J. Chem. Phys.* **117**, 6982 (2002).
- ³²J. Li, X. Li, H. J. Zhai, and L. S. Wang, *Science* **299**, 864 (2003).
- ³³H. Hakkinen, B. Yoon, U. Landman, X. Li, H. J. Zhai, and L. S. Wang, *J. Phys. Chem. A* **107**, 6168 (2003).
- ³⁴X. Li, B. Kiran, J. Li, H. J. Zhai, and L. S. Wang, *Angew. Chem., Int. Ed.* **41**, 4786 (2002).
- ³⁵B. Kiran, X. Li, H. J. Zhai, L. F. Cui, and L. S. Wang, *Angew. Chem., Int. Ed.* **43**, 2125 (2004).
- ³⁶D. Fischer, W. Andreoni, A. Curioni, H. Gronbeck, S. Burkart, and G. Gantefor, *Chem. Phys. Lett.* **361**, 389 (2002).
- ³⁷S. Buckart, G. Gantefor, Y. D. Kim, and P. Jena, *J. Am. Chem. Soc.* **125**, 14205 (2003).
- ³⁸X. Wang and L. Andrews, *J. Am. Chem. Soc.* **123**, 12899 (2001).
- ³⁹X. Wang and L. Andrews, *J. Phys. Chem. A* **106**, 3744 (2002).
- ⁴⁰L. Andrews and X. Wang, *J. Am. Chem. Soc.* **125**, 11751 (2003).
- ⁴¹L. S. Wang, H. S. Cheng, and J. Fan, *J. Chem. Phys.* **102**, 9480 (1995).
- ⁴²L. S. Wang and H. Wu, in *Advances in Metal and Semiconductor Clusters, Cluster Materials*, Vol. 4, edited by M. A. Duncan (Jai, Greenwich, 1998), pp. 299-343.
- ⁴³K. P. Huber and G. Herzberg, *Molecular Spectra and Molecular Structure. IV. Constants of Diatomic Molecules* (Van Nostrand Reinhold, New York, 1979).
- ⁴⁴G. A. Bishea and M. D. Morse, *J. Chem. Phys.* **95**, 5646 (1991).
- ⁴⁵J. P. Perdew and Y. Wang, *Phys. Rev. B* **45**, 13244 (1992).
- ⁴⁶E. van Lenthe, E. J. Baerends, and J. G. Snijders, *J. Chem. Phys.* **99**, 4597 (1993).
- ⁴⁷ADF 2002, SCM, Theoretical Chemistry, Vrije Universiteit, Amsterdam, Netherlands (www.scm.com).
- ⁴⁸D. W. Boo, Y. Ozaki, L. H. Andersen, and W. C. Lineberger, *J. Phys. Chem. A* **101**, 6688 (1997).
- ⁴⁹T. Leisner, S. Vajda, S. Wolf, L. Woste, and R. S. Berry, *J. Chem. Phys.* **111**, 1017 (1999).
- ⁵⁰R. Wesendrup, T. Hunt, and P. Schwerdtfeger, *J. Chem. Phys.* **112**, 9356 (2000).
- ⁵¹C. W. Bauschlicher, Jr., S. R. Langhoff, and H. Patridge, *J. Chem. Phys.* **91**, 2412 (1989).
- ⁵²S. Wolf, G. Sommerer, S. Rutz, E. Schreiber, T. Leisner, L. Woste, and R. S. Berry, *Phys. Rev. Lett.* **74**, 4177 (1995).